Title	Performances of oscillating radial collimator for the Fermi chopper spectrometer 4SEASONS at J-PARC
Author(s)	Nakamura Mitsutaka, Kambara Wataru, Iida Kazuki, Kajimoto Ryoichi, Kamazawa Kazuya, Ikeuchi Kazuhiko, Ishikado Motoyuki, Aoyama Kazuhiro
Citation	Physica B; Condensed Matter,551,p.480-483
Text Version	Accepted Manuscript
URL	https://jopss.jaea.go.jp/search/servlet/search?5059697
DOI	https://doi.org/10.1016/j.physb.2018.05.028
Right	© 2018. This manuscript version is made available under the CC-BY-NC-ND 4.0 license http://creativecommons.org/licenses/by-nc-nd/4.0/

Performances of oscillating radial collimator for the Fermi chopper spectrometer 4SEASONS at J-PARC

Mitsutaka Nakamura[a,*], Wataru Kambara[a], Kazuki Iida[b], Ryoichi Kajimoto[a], Kazuya Kamazawa[b], Kazuhiko Ikeuchi[b], Motoyuki Ishikado[b], Kazuhiro Aoyama[a]

[a]*Materials and Life Science Division, J-PARC Center, Japan Atomic Energy Agency, Tokai, Ibaraki, 319-1195, Japan*
[b]*Neutron Science and Technology Center, Comprehensive Research Organization for Science and Society, Tokai, Ibaraki, 319-1106, Japan*

Abstract

A novel operation pattern is introduced into the oscillating radial collimator for the Fermi chopper spectrometer 4SEASONS at the Materials and Life Science Experimental Facility in J-PARC. This pattern is shown to suppress shadows originating from shielding blades of the radial collimator. We also report the transmission property of the oscillating radial collimator for 4SEASONS, based on an investigation of the scattered intensities from polycrystalline samples of different diameter.

Keywords: Oscillating radial collimator, Chopper spectrometer, Inelastic neutron scattering

1. Introduction

There has recently been an increasing need for inelastic neutron scattering (INS) measurements [1, 2] in special sample environment such as strong magnetic fields and high temperatures. To obtain high-quality data, the unwanted scatterings originating from these sample environment equipments should be suppressed as much as possible. A radial collimator with a lot of shielding blades radially arranged at regular intervals has conventionally been used to eliminate these unwanted scatterings [3, 4]. It is also typical to oscillate the shielding blades at a certain speed because the blades themselves cause shadows in the signal to be detected.

We have developed two types of oscillating radial collimators for chopper spectrometers at the Materials and Life Science Experimental Facility (MLF) at the Japan Proton Accelerator Research Complex (J-PARC) [5]. One type uses commercially available Gd_2O_3 sheets as shielding blades, and is employed in the AMATERAS [6] installed at beamline 14 (BL14) in the MLF; the other is made of Cd-plated aluminum sheets, as used for 4SEASONS [7] at BL01. The Gd_2O_3 radial collimator provides sufficient performance in experiments with AMATERAS utilizing incident energy (E_i) between 1 and 80 meV. However, the shielding property of Gd_2O_3 worsens for energies above several hundred meV, as the large incoherent scatterings from the polymer substrate adversely affect the signal to be detected. In 4SEASONS, which is designed for measurements at energies up to 300 meV, the hydrogen-free metal sheet is chosen for the substrate of a radial collimator blade. This paper describes the newly introduced operation pattern and evaluates the performance of the oscillating radial collimator specialized for 4SEASONS (4SEASONS-ORC).

2. The shift-mode operation

To begin with, let us introduce the design parameters of the 4SEASONS-ORC [5]. It has an inner radius (R_1) of 210 mm, an outer radius (R_2) of 400 mm, an angular separation α of 2.5°, and a blade height of 482 mm. The diameter of the visible sample b_0 is estimated to be 19.3 mm based on the relation $b_0 = \alpha R_1 R_2/(R_2 - R_1)$. The design of the neutron guide system for 4SEASONS was optimized by assuming a sample size of 20 mm × 20 mm [7, 8], which is almost equivalent to the b_0 value of the 4SEASONS-ORC. As might be expected, this b_0 is much smaller than the inner diameters of the typical sample environments ($\gtrsim$ 50 mm). The shielding blades cover the range from −45° to +135° in a horizontal direction; however, none are installed along the direct beam path. The oscillation of a shielding blade is

*Corresponding author. Tel: +81 29 284 3198
Email address: mitsutaka.nakamura@j-parc.jp (Mitsutaka Nakamura)

driven by a stepper motor, where accurate position control is achieved with a programmable logic controller (PLC). Linear motion by a ball screw directly connected to the stepper motor is converted into rotary motion by a crossed roller bearing.

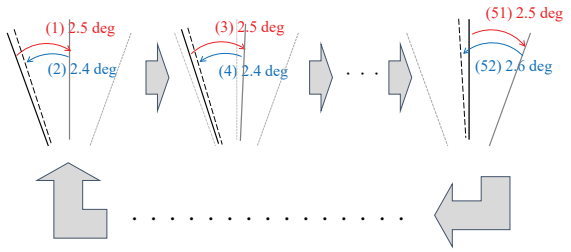

Figure 1: Schematic illustration representing shift-mode operation. The angular separation between neighboring blades is assumed to be 2.5° in this figure. The detailed oscillation sequence is described in the text.

Generally, the oscillating angle of a radial collimator must be an integer multiple of an angular separation α; otherwise, the blades cause shadows in a certain angular range. However, it should be noted that shadows inevitably exist, even if the above conditions are satisfied. This is because there exists a *dead-time* when a blade changes its direction of movement, which causes a series of shadows in the signal to be detected. To prevent these inevitable shadows we need to introduce a new operation pattern into the 4SEASONS-ORC, even though it already achieves a considerably short dead-time (20 ms) by virtue of the rigidity of the direct motor drive ball screw. We refer to this new operational pattern as the *shift-mode*. The detailed movements of the shielding blades in shift-mode are schematically illustrated in Fig. 1. The red arrows correspond to the forward direction and the blue to the backward one. The angular separation α is assumed to be 2.5° in this figure. At the start of operation, one blade moves in a forward direction by an oscillating angle equal to α (= 2.5°) and returns in a backward direction by an angle slightly *less than* the oscillating one. In Fig. 1, the angle in the backward direction is 2.4°, meaning that the shift amount per one reciprocation is 0.1°. When the total shift amount reaches the value of angular separation (= 2.5°), the amount of movement in the backward direction is changed such that the angle is slightly *greater than* the oscillating one, which is set to be 2.6° in Fig. 1. Consequently, the gradual shifting of the dead-center position will bring about a homogeneous signal.

The benefit of shift-mode operation is displayed in Fig. 2. A white neutron beam was irradiated onto the vanadium sample and the scattered neutrons were

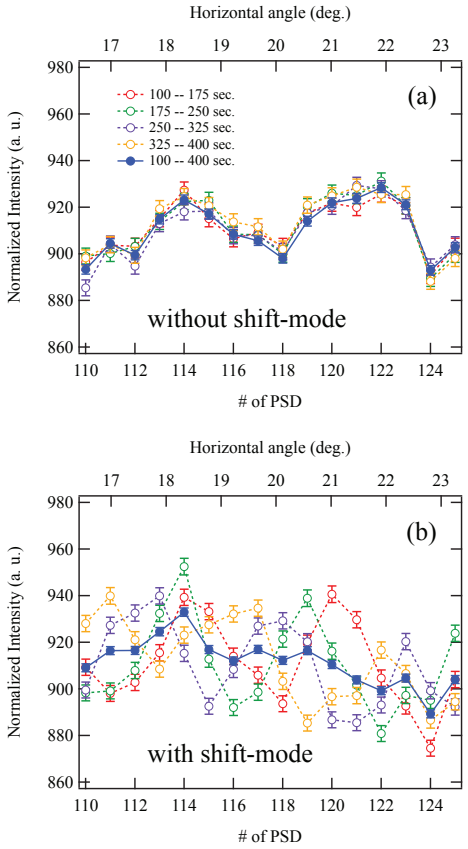

Figure 2: The intensity distributions along the horizontal direction. The incoherent scatterings from vanadium are detected through the 4SEASONS-ORC by ^{3}He position sensitive detectors (a) without and (b) with shift-mode operation. The oscillating speed and angle are 0.33°/s and 2.5°, respectively. Each exposure time after the start of measurement is indicated in the figure.

detected by ^{3}He position sensitive detectors (PSD) with dimensions of ϕ19 mm × 2,500 mm, covering the horizontal-scattering-angle region from −35.3° to +90.7°. In Figs. 2(a) and (b), the oscillating speed and angle were set to 0.33°/s and 2.5°, respectively. The shift amount per one reciprocation was 0.1°. Each exposure time after the start of measurement is indicated in the figures. Over a period of 75 seconds, the shielding blades reciprocate 5 times, — i.e., shift amounts accumulate to 0.5° during shift-mode operation. Each intensity was accumulated in the time-of-flight region from 10,000 μs to 20,000 μs and integrated in the region of ±15° in the vertical direction. The difference in the exposure time was normalized by the incident proton current into the neutron target during the exposure time, and solid-angle correction was also performed. These data reduction processes were completed by us-

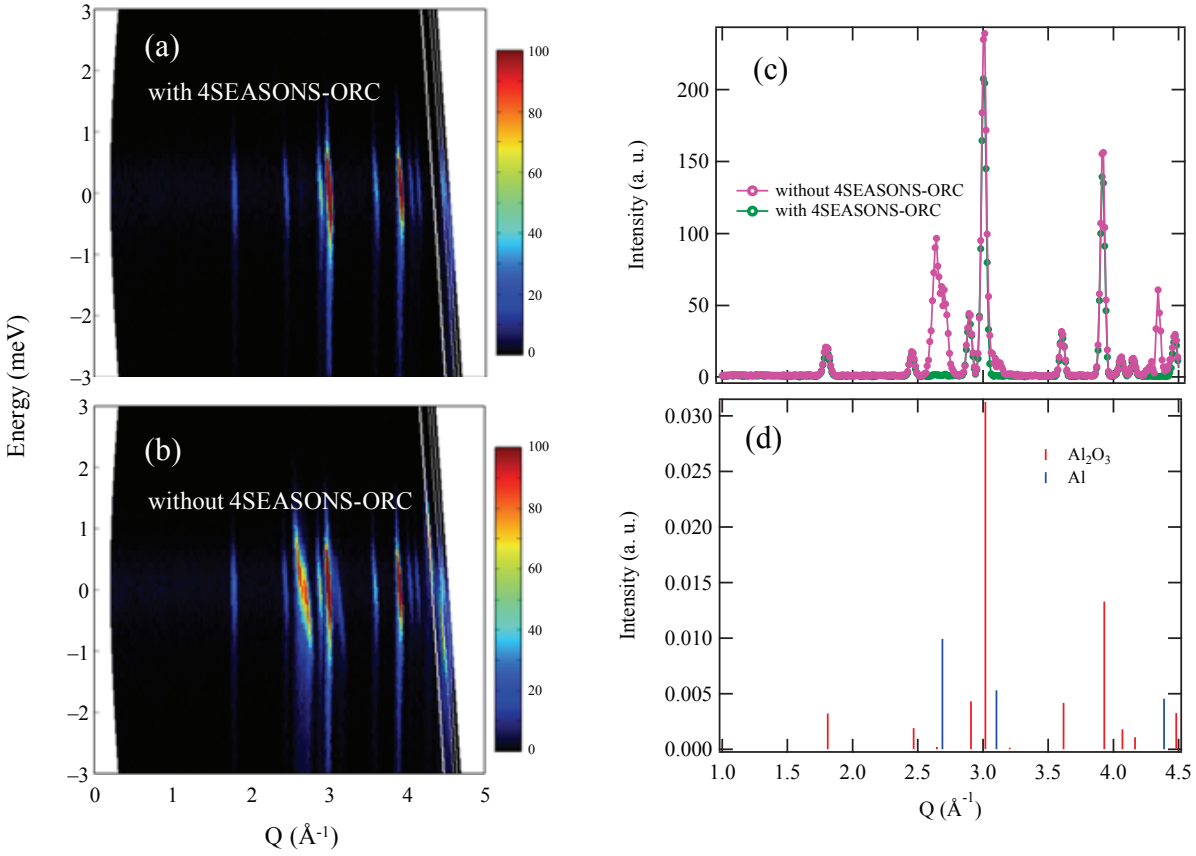

Figure 3: The $S(Q, E)$ maps of the Al_2O_3 rod at around the elastic region (a) with and (b) without 4SEASONS-ORC. The diameter of the sample rod is 5 mm and E_i is 20.9 meV for both measurements. (c) Comparison of elastic spectra sliced at $E = 0 \pm 0.1$ meV. (d) The calculated diffraction spectra of Al and Al_2O_3 in powder forms.

ing the Utsusemi suite [9]. The horizontal axis of Fig. 2 is the PSD number of 4SEASONS, which corresponds to the horizontal-scattering-angle range from +16.53° to +23.24°. As clearly shown in Fig. 2(a), intensity gaps appear every seven PSDs. These angular intervals of ~ 2.6° correspond to the angular separation α of 4SEASONS-ORC. On the other hand, Fig. 2(b) demonstrates that the intensity gaps are gradually shifted over time, and the homogeneity of the detected signals is improved. Figure 2(a) suggests that an unevenness of about 5% with respect to the baseline intensity can be induced when the shift-mode is not used. Consequently, shift-mode operation is surely effective in the case where data with an intensity unevenness of 5% are still insufficient to present conclusive evidence.

3. Transmission performance of the 4SEASONS-ORC

Next, we shall discuss the neutron transmission property of the 4SEASONS-ORC. To evaluate its performance, we have investigated the Bragg peak intensities from polycrystalline Al_2O_3 rods with and without 4SEASONS-ORC. We prepared six Al_2O_3 rods with diameters of 5, 10, 15, 20, 30, and 40 mm. Each sample was set into the top-loading cryostat conventionally used at 4SEASONS where the diameter of inner vacuum chamber (IVC) is 99 mm. The scattering signals from the cryostat should be included in the case of measurements without the 4SEASONS-ORC, and the shift-mode operation was used in the measurements with the 4SEASONS-ORC. The incident neutron energies were set to 13.5, 20.9, 36.7, and 80.7 meV using the so-called Multi-E_i method [10]. Figures 3(a) and (b) show the dynamical structure factor $S(Q, E)$ of a polycrys-

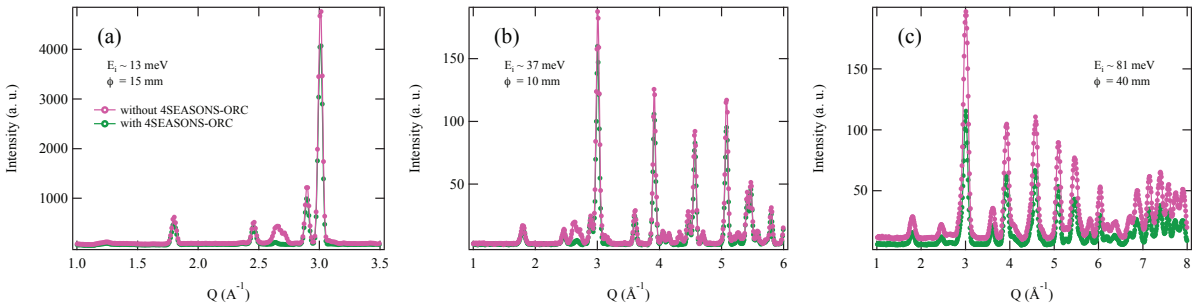

Figure 4: Other comparative examples of elastic spectra : (a) $E_\mathrm{i} \sim 13$ meV and $\phi = 15$ mm; (b) $E_\mathrm{i} \sim 37$ meV and $\phi = 10$ mm; (c) $E_\mathrm{i} \sim 81$ meV and $\phi = 40$ mm.

talline Al_2O_3 rod with [Fig. 3(a)] and without [Fig. 3(b)] 4SEASONS-ORC. The diameter of rod ϕ is 5 mm and E_i is 20.9 meV for both cases. Each elastic spectrum sliced at $E = 0 \pm 0.1$ meV is compared in Fig. 3(c). The calculated diffraction spectra for both Al and Al_2O_3 in powder form are plotted in Fig. 3(d). It is obvious that unwanted scatterings from the cryostat are almost completely eliminated by use of the 4SEASONS-ORC. Other comparative examples are displayed in Fig. 4. We would like to emphasize that the scattering angles of Bragg peaks vary depending on E_i. In fact, the angular dependence of the transmission property of the 4SEASONS-ORC can be surveyed by investigating the E_i dependence of a specific Bragg peak intensity.

The ratio of the Bragg peak intensity with the 4SEASONS-ORC to that without is represented as a function of diameter in Fig. 5. The intensity ratios of the Bragg peaks at $Q = 1.8$ Å^{-1} and $Q = 3.9$ Å^{-1} are shown in Figs. 5(a) and (b), respectively. As shown in Fig. 3, there is no contamination from the scattering of Al at around $Q = 1.8$ Å^{-1} and 3.9 Å^{-1}. Each Bragg peak was fitted by a Gaussian function and a linear baseline and the intensity was taken as the peak value of a fitted Gaussian. The intensity ratio, $I_{with}/I_{without}$, in Fig. 5 can be theoretically represented as

$$\frac{I_{with}}{I_{without}} = \frac{\int_0^r rV(r)dr}{\int_0^r rdr}, \tag{1}$$

where r is the radius of a sample and $V(r)$ the Copley's visibility function [3]. The $V(r)$ formula is written as

$$V(r) = \frac{2t_0}{\pi}\left[\Psi_b - \frac{\Psi_\delta \delta}{b_0} + \frac{r(\cos\Psi_b - \cos\Psi_\delta)}{b_0}\right], \tag{2}$$

where

$$\Psi_\delta = \sin^{-1}(\delta/r), \qquad \delta \le r, \tag{3}$$
$$= \pi/2, \qquad \delta \ge r, \tag{4}$$

and

$$\Psi_b = \sin^{-1}(b_0/r), \qquad b_0 \le r, \tag{5}$$
$$= \pi/2, \qquad b_0 \ge r. \tag{6}$$

Here, 2δ is the thickness of a blade (= 0.15 mm for 4SEASONS-ORC). Using the design parameters of the 4SEASONS-ORC, the maximum transmission of a collimator (t_0) and the maximum impact parameter (b_0) [3] are set to be 1 and 19.3 mm, respectively. Accordingly, the visibility function of Eq. (2) for the 4SEASONS-ORC can be simply given by

$$V(r) = \frac{2}{\pi}\left[\frac{\pi}{2} - \frac{r}{b_0}\right], \tag{7}$$
$$= 1 - \frac{2}{\pi}\left(\frac{r}{b_0}\right), \tag{8}$$

where we assume that δ is negligible in the calculation. Thus, the intensity ratio can be analytically solved as

$$\frac{I_{with}}{I_{without}} = 1 - \frac{4}{3\pi}\left(\frac{r}{b_0}\right). \tag{9}$$

As shown in Fig. 5, the calculated intensity ratio is found to well-reproduce the experimental results.

The signal-to-noise ratios (SNRs) of the Bragg peaks at $Q = 1.8$ Å^{-1} and $Q = 3.9$ Å^{-1} are estimated in Figs. 6(a) and (b), respectively. The Bragg peak was also fitted by a Gaussian function and a linear baseline. Each SNR was taken as the ratio between the peak value of a fitted Gaussian and the height of a fitted baseline. For a sample with a diameter under 10 mm, the

4SEASONS-ORC can improve the SNR because the parasitic scatterings, which give rise to constant background, are effectively reduced compared with the peak signal.

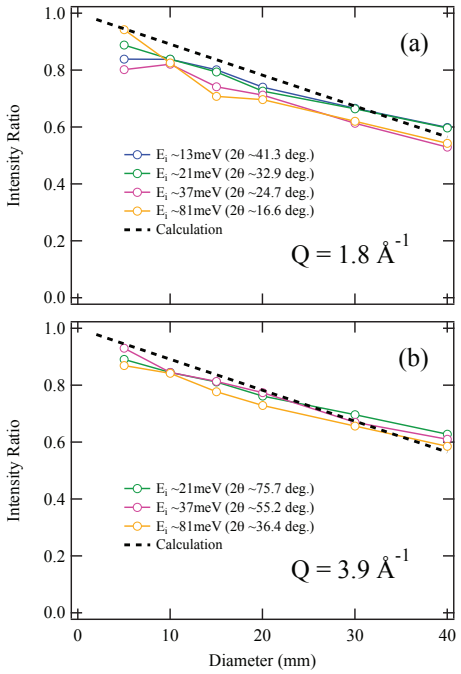

Figure 5: The ratio of the Bragg peak intensity with the 4SEASONS-ORC to that without as a function of diameter. The experimental results for Bragg peaks at (a) Q = 1.8 Å^{-1} and (b) Q = 3.9 Å^{-1} are plotted. The calculated intensity ratio is also plotted.

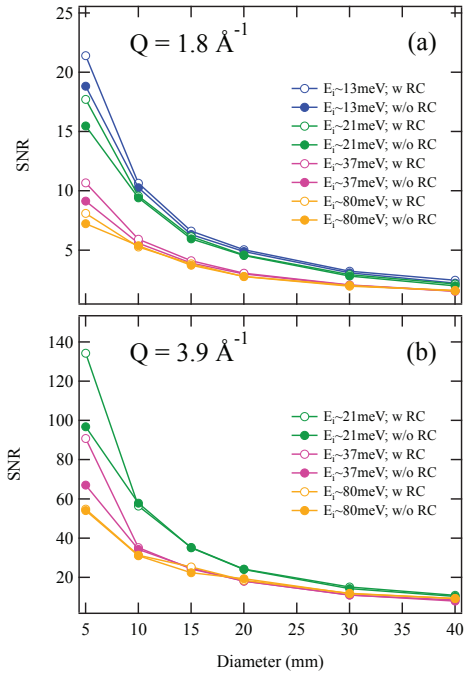

Figure 6: The signal-to-noise ratios (SNRs) of the Bragg peaks at (a) Q = 1.8 Å^{-1} and (b) Q = 3.9 Å^{-1} as functions of diameter. Open symbol: SNR with 4SEASONS-ORC. Closed symbol: SNR without 4SEASONS-ORC.

4. Conclusion

We have introduced a new operation pattern (shift-mode) of a radial collimator into the Fermi chopper spectrometer 4SEASONS. The shift-mode can bring about more homogeneous signals, preventing shadows due to the shielding blade itself. Both the transmission property and the signal-to-noise ratio were evaluated by investigating the Bragg peak intensities from polycrystalline Al_2O_3 rods of various diameters. An excellent performance was shown irrespective of scattering angle or Q position.

Acknowledgments

We are grateful to the technical support team of J-PARC Center. The experiments on 4SEASONS were performed under the user programs 2015I0001 and 2016I0001.

[1] M.B. Stone, J.L. Niedziela, M.J. Loguillo, M.A. Overbay, D.L. Abernathy, Rev. Sci. Instrum. 85 (2014) 085101.
[2] G. Günther, M. Russina, Nucl. Instrum. Methods Phys. Res. Sect. A 828 (2016) 250.
[3] J.R.D. Copley, J.C. Cook, Nucl. Instrum. Methods Phys. Res. Sect. A 345 (1994) 313.
[4] A.F. Wright, M. Berneron, S.P. Heathman, Nucl. Instrum. Methods 180 (1981) 655.
[5] M. Nakamura, Y. Kawakita, W. Kambara, K. Aoyama, R. Kajimoto, K. Nakajima, S. Ohira-Kawamura, K. Ikeuchi, T. Kikuchi, Y. Inamura, K. Iida, K. Kamazawa, M. Ishikado, JPS Conf. Proc. 8 (2015) 036011.
[6] K. Nakajima, S. Ohira-Kawamura, T. Kikuchi, M. Nakamura, R. Kajimoto, Y. Inamura, N. Takahashi, K. Aizawa, K. Suzuya, K. Shibata, T. Nakatani, K. Soyama, R. Maruyama, H. Tanaka, W. Kambara, T. Iwahashi, Y. Itoh, T. Osakabe, S. Wakimoto, K. Kakurai, F. Maekawa, M. Harada, K. Oikawa, R. E. Lechner, F. Mezei, M. Arai, J. Phys. Soc. Jpn. 80 (2011) SB028.
[7] R. Kajimoto, M. Nakamura, Y. Inamura, F. Mizuno, K. Nakajima, S. Ohira-Kawamura, T. Yokoo, T. Nakatani, R. Maruyama, K. Soyama, K. Shibata, K. Suzuya, S. Sato, K. Aizawa, M. Arai, S. Wakimoto, M. Ishikado, S. Shamoto, M. Fujita, H. Hiraka, K. Ohoyama, K. Yamada, C.H. Lee, J. Phys. Soc. Jpn. 80 (2011) SB025.
[8] R. Kajimoto, K. Nakajima, M. Nakamura, K. Soyama, T. Yokoo, K. Oikawa, M. Arai, Nucl. Instrum. Methods Phys. Res. Sect. A 600 (2009) 185.

[9] Y. Inamura, T. Nakatani, J. Suzuki, T. Otomo, J. Phys. Soc. Jpn. 82 (2013) SA031.
[10] M. Nakamura, R. Kajimoto, Y. Inamura, F. Mizuno, M. Fujita, T. Yokoo, M. Arai, J. Phys. Soc. Jpn. 78 (2009) 093002.